4-20-2009

Characterization of gold contacts in GaAs-based molecular devices: Relating structure to electrical properties

Patrick D. Carpenter
School of Electrical and Computer Engineering, Birck Nanotechnology Center, Purdue University, pdcarpen@purdue.edu

Saurabh Lodha
School of Electrical and Computer Engineering, Birck Nanotechnology Center, Purdue University

David B. Janes
Purdue University, david.b.janes.1@purdue.edu

Amy V. Walker
Washington University

Chemical Physics Letters 472 (2009) 220–223

Contents lists available at ScienceDirect

Chemical Physics Letters

journal homepage: www.elsevier.com/locate/cplett

Characterization of gold contacts in GaAs-based molecular devices: Relating structure to electrical properties

Patrick D. Carpenter [a], Saurabh Lodha [a], David B. Janes [a,*], Amy V. Walker [b,*]

[a] School of Electrical and Computer Engineering, Birck Nanotechnology Center, Purdue University, West Lafayette, IN 47907, USA
[b] Department of Chemistry, Campus Box 1134, Washington University in St. Louis, One Brookings Drive, St. Louis, MO 63130, USA

ARTICLE INFO

Article history:
Received 25 October 2008
In final form 5 March 2009
Available online 11 March 2009

ABSTRACT

Au/octadecanethiol/GaAs devices were prepared using different metallization conditions: direct deposition at 77 K and 300 K samples, and indirect deposition (Ar backfilling). Time-of-flight secondary ion mass spectrometry data indicate that ~4x and ~2x more gold penetrates through the SAM after direct deposition at 300 K and 77 K, respectively, than under Ar backfill conditions. However, these devices have significantly different conductances: Ar-backfill and 77 K samples have ~200x and ~70x, respectively, larger conductances than 300 K devices. An electrostatic model has been developed to explain the very large conductance changes due to small differences in device structure.

1. Introduction

The field of molecular electronics in recent years has attracted considerable interest for continued scaling of very large-scale integration (VLSI) technology because it has the potential to produce high density, nanometer scale electronic devices. While most studies of molecular devices have focused on metal–molecule–metal structures [1,2], metal–molecule–semiconductor devices are also attractive since the substrates employed are technologically relevant. Further the doping, energy bands and surface properties of semiconductors can be used to tailor device performance.

A metal–molecule–metal or metal–molecule–semiconductor construct consists of the top metal–molecule contact, a molecular core and the molecule–substrate contact. In the last few years it has become clear that the contact-molecule geometry [3–8] and binding [1,2,7,9], the molecule–electrode distance [3,9,10] and the dynamics of the junction [11] are critical factors that determine the device conductance. Thus a key challenge in molecular device fabrication is to obtain a stable and reproducible top contact to the nanometer-scale molecular layer. A number of techniques have been employed to make metal contacts to molecular layers; including lift-off Au pads [12], mercury droplets [13], break junctions [14], and scanning probe tips [15]. These methods are unsuitable for large-scale integration, so additional techniques are of interest. The physical vapor deposition of metal contacts on molecular layers adsorbed on metal surfaces has also been extensively studied [16–20]. It remains unclear, however, how the structure of the vapor-deposited metallic contact affects the electronic transport properties of the molecular device.

In this Letter, we compare the physical and electronic properties of Au/octadecanethiol/p^+-GaAs structures prepared using two different Au evaporation techniques: direct evaporative deposition on 300 K and 77 K substrates, and indirect deposition ('Ar backfilling'). We show that the structure of the gold top contact can be controlled via the substrate temperature and kinetic energy of the impinging gold atoms. Furthermore, we observe that small changes in the amount of gold penetration through the octadecanethiol monolayer lead to significant changes in the conductance of the device. To explain these data, we have developed a model in which these devices consist of three different conducting regions, each with a different *current density–voltage* relationship.

2. Experimental details

The preparation of the self-assembled monolayers of octadecanethiol (ODT) on p^+-GaAs ($N_A = 1 \times 10^{19}$ cm^{-3}) and the Au/SAM/GaAs device fabrication procedure have been discussed in detail previously [21–23]. The prepared SAMs were characterized using transmission Fourier Transform Infrared (FTIR) spectroscopy, single wavelength ellipsometry, atomic force microscopy and time-of-flight secondary ion mass spectrometry (TOF SIMS) to ensure that the monolayers formed were free of impurities.

Three different evaporation conditions were employed to deposit 10–15 nm thick Au top contacts. Two direct evaporation protocols were used, in which the SAM/GaAs sample was maintained at either 300 K or 77 K and the gold deposited at 0.1 nm/s. The third technique ('Ar backfill') was performed in a modified thermal evaporator, which was backfilled with Ar (8 mtorr) to reduce the kinetic energy of Au atoms impinging on the sample. The samples

* Corresponding authors. Fax: +1 765 494 0811 (D.B. Janes)/+1 314 935 4481 (A.V. Walker).
E-mail addresses: janes@ecn.purdue.edu (D.B. Janes), walker@wustl.edu (A.V. Walker).

0009-2614/$ - see front matter © 2009 Elsevier B.V. All rights reserved.
doi:10.1016/j.cplett.2009.03.019

were kept out of line-of-sight of the evaporation source to prevent damage from direct radiative heating. For this method, the deposition rate was ~0.0125 nm/s.

To investigate the structure of the Au/ODT/GaAs devices, unpatterned samples (~1 cm^2) were prepared with 12 nm Au layers and examined using transmission FTIR spectroscopy and TOF SIMS. A lightly-doped GaAs substrate was employed to ensure transmission of IR light through the Au/ODT/GaAs samples.

To study the electrical transport of the Au/ODT/p^+-GaAs devices, samples were prepared in which the ODT SAM was formed in a ~6 μm diameter opening in a SiO_2 layer on the GaAs surface. For these measurements, ~15 nm of Au was deposited on ODT/p^+-GaAs samples for each of the direct evaporation conditions. For the Ar-backfill Au/ODT/p^+-GaAs samples, as well as for the Au/p^+-GaAs control, the first ~12 nm was deposited under Ar-backfill conditions. To obtain a thicker contact layer suitable for electrical measurements, additional Au was deposited using direct evaporation at 300 K.

3. Results and discussion

The IR spectra of the ODT/GaAs samples display peaks corresponding to the symmetric (d^+) and asymmetric (d^-) CH_2 stretches at 2849 and 2917 cm^{-1}, respectively (Fig. 1) [24]. After direct deposition of Au at 300 K, the intensities of the CH_2 stretches have greatly decreased and broadened, indicating that there is significant disturbance of the monolayer. This could be attributed to either conformational disordering of the monolayer or desorption of the monolayer upon Au evaporation. However, it seems unlikely that desorption of the monolayer is occurring since alkanethiolate SAMs adsorbed on GaAs (001) are stable to at least 393 K [25]. In contrast, for the 77 K direct evaporation sample the IR spectra indicate that there is little or no disturbance of the monolayer structure, with the peak positions and intensities remaining approximately the same as those observed for the bare monolayer. For the Ar backfill sample, the IR data show that there is some conformational disorder induced by the backfill Au deposition. In Fig. 1, it can be clearly seen that there appears to be a long, low-wavenumber tail associated with the asymmetric (d^-) CH_2 stretch, indicative of the formation of gauche defects at the terminal methyl group [24]. The intensity of the symmetric (d^+) CH_2 stretch also decreases by approximately 18%, suggesting that the monolayer has undergone some disordering. Finally, the symmetric (d^+) and asymmetric (d^-) CH_2 stretches broaden slightly, confirming that there is a small amount of conformational disorder induced by the Ar backfill deposition method.

For all samples studied, ions characteristic of the monolayer are observed in the positive and negative TOF SIMS spectra, for example $Ga_xS_y(CH_2)_z^+$, $As_xS_y(CH_2)_z^+$. These indicate that the SAM does not desorb from the surface upon Au deposition and that there are regions in which ODT is bound to As or Ga sites on the GaAs surface [26,27]. In addition, after Au deposition, ions containing Au and S, such as $AuSH_2^+$ and $AuS(CH_2)_x^+$, are observed, indicating that Au penetrates through the SAM to the GaAs/S interface [19]. In the negative ion mass spectra we observe ions of the form $Au_xGa_yS_z^-$ and $Au_xAs_yS_z^-$ confirming that Au has penetrated through the monolayer to the GaAs/S interface (data not shown). Fig. 2 displays an example of the data obtained: high resolution positive ion mass spectra centered at *m/z* 231. We note that secondary ion intensities are dependent on the material ('matrix') that surrounds the structure of interest. In this case, the matrix is similar for all three deposition conditions, and so the intensities can be compared to obtain the relative amounts of Au that penetrate through the SAM to the GaAs/S interface [20]. In Fig. 2, it can be clearly seen that more Au has penetrated through the 300 K and 77 K direct-deposited samples than through the Ar backfill sample. From the relative intensities of the $AuSH_2^+$ ions we estimate that the amount of Au penetration is four times larger for direct evaporation at 300 K than for Ar backfill evaporation. The amount of Au that penetrates through the monolayer for 77 K direct deposition is approximately twice that for an Ar backfill sample. Finally, we note that analysis of the intensities of other Au and S containing ions give similar results.

Taken together, the IR and TOF SIMS data indicate that the ODT monolayer is disordered after direct Au evaporative deposition at 300 K and that Au penetrates to the GaAs/S interface. Under Ar backfill conditions, the monolayer is disordered slightly with gauche defects forming at the methyl terminal group. Ar backfill also results in the least amount of Au penetration through the monolayer to the S/GaAs interface. In contrast, after deposition of Au at 77 K there is little, or no, conformational disordering of the monolayer but more Au penetrates through the SAM. For all deposition conditions ions characteristic of the SAM adsorbed to Ga and As surface sites are observed indicating that there are areas in the devices where Au has not penetrated through the ODT SAM to the GaAs/S interface.

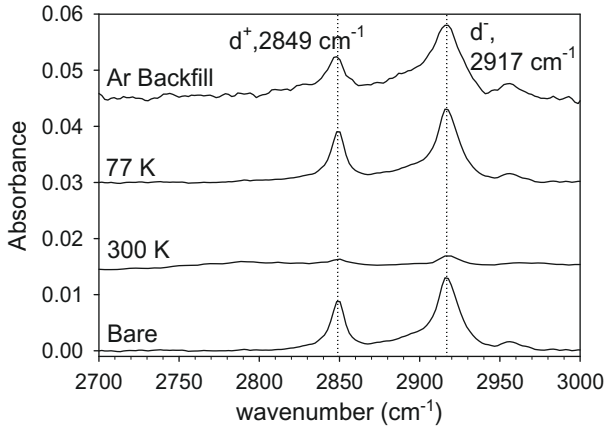

Fig. 1. Transmission IR spectra of the bare monolayer and after deposition of 120 Å Au using the various experimental conditions. Resolution: 8 cm^{-1}; no. of scans averaged 256.

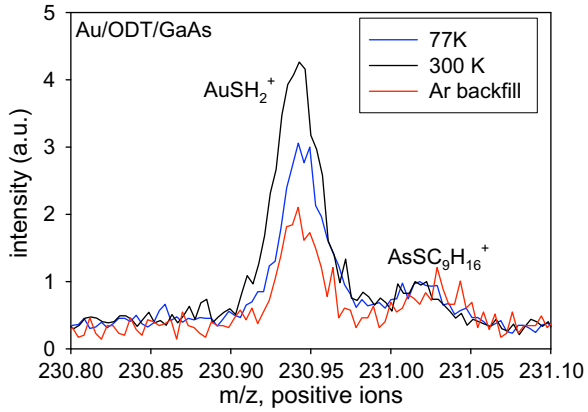

Fig. 2. TOF SIMS high resolution positive ion mass spectra centered at *m/z* 231 for Au/ODT/p^+-GaAs samples fabricated using Ar backfill, and 77 K and 300 K direct evaporation of the top Au contact. The peak intensities are normalized to the peak intensity of the $AsSC_9H_{16}^+$ ion to make clear the changes in ion intensities upon Au deposition. Primary ion: Bi^+; kinetic energy 25 keV; primary ion dose 1×10^8 ions cm^{-2}; area of analysis (100×100) μm^2.

Fig. 3 displays representative current–voltage (I–V) data for Au/ODT/p^+-GaAs devices produced using the three different Au deposition conditions as well as for a control sample, Au/p^+-GaAs. The Ar backfill device has the highest conductivity, followed by the 77 K device, which in turn conducts better than the 300 K direct deposition device. The control device has the lowest conductivity of all four devices. We note that similar results are reported for the conductance of a variety of alkanethiols in Au/SAM/p^+-GaAs devices [22,23]. The model employed in the present study is consistent with the reported trends in conductance. The maximum observed current density for the Au/ODT/p^+-GaAs devices ($\sim 10^5$ A cm^{-2}) corresponds to a current per molecule of $\sim$1 nA (at typical molecular packing densities of $\sim 5 \times 10^{14}$ cm^{-2} [28]), or an average resistance of $\sim 10^9$ Ω, which is in agreement with reported resistances for alkanethiolates in metal–molecule–metal and metal–molecule–semiconductor structures ($\sim 10^7$ to 10^{10} Ω/molecule) [1]. X-ray photoelectron spectroscopy (XPS) measurements indicated that the surface coverage of the ODT SAM is consistent with a dense monolayer. Previous studies using the same deposition methods and alkanethiol have verified the formation of a well-ordered monolayer of surface density of 21.2 Å^2/molecule [24]. Such a monolayer is space filling and therefore blocks any unterminated surface sites from subsequent reactions. This is consistent with the observation of significantly lower oxidation of the GaAs surface [24], and resistance to chemical attack by both bases [27] and acids [29] of the SAM-covered GaAs surface with respect to the bare GaAs.

The I–V data provide insights into the barriers limiting conduction in the various devices. The I–Vs of the control and the 300 K samples share many similarities, including their rectification ratios ($\sim$9 and 8, respectively). The rectification in these devices is consistent with the expected barrier height for the Au/p+-GaAs Schottky barrier [21]. The measured forward-bias conductance of the control device is consistent with a thermionic field emission (TFE) model for a Schottky diode with a doping density of $\sim 1 \times 10^{19}$ cm^{-3} and a barrier height of $\sim$0.4 eV for this structure [30,31]. The Ar backfill and the 77 K devices show more symmetric I–Vs, with rectification ratios of $\sim$1 in both cases. Together with the relatively high current densities in these devices, these observations indicate a relatively low barrier height in these devices. For high substrate doping densities, much of the intrinsic electrostatic potential can be dropped across the molecular layer, leading to a low semiconductor barrier height [21,22]. Fig. 4 shows the effects of electrostatic potential drops and changes in barrier heights for both Au/p^+-GaAs and Au/ODT/p^+-GaAs devices on the band diagrams.

Since Au penetrates through ODT to the S/GaAs interface, these devices can be considered to be a mix of regions of Au/p^+-GaAs Schottky contacts and Au/ODT/p^+-GaAs structures. These areas represent parallel conduction paths with different conductances per unit area. The Au/ODT/p^+-GaAs areas are expected to conduct better than Au/p^+-GaAs regions for two reasons. First, in a Au/ODT/p^+-GaAs region, the semiconductor barrier can be significantly smaller and correspondingly more transparent, than in a region in which gold is in contact with the GaAs substrate [21–23]. In this case, the limiting conductance is due to the transmission coefficient through the molecular layer. Second, the covalent binding between ODT and the GaAs surface provides a relatively strong coupling to the GaAs contact, which increases the device conductance [21–23]. Hence, the conductance levels observed for the various devices (Fig. 3) indicate that the amount of Au penetration progressively increases from the Ar backfill sample to the 77 K direct evaporation sample to the 300 K direct evaporation sample, in agreement with the TOF SIMS data. However, the ratio between the device conductances ($\sim$1/$\sim$70/$\sim$200, 300 K/77 K/Ar backfill) is much larger than the relative amounts of Au penetration inferred from the TOF SIMS data ($\sim$4/$\sim$2/$\sim$1, 300 K/77 K/Ar backfill) (Fig. 2). Furthermore, it is not possible to construct the measured I–V relationship for the 300 K sample from a weighted linear combination of the data for the Ar backfill device and the control sample.

To qualitatively explain the large variation of conductance with apparently small changes in device structures, we propose a model in which there are three types of conducting regions, each with a different current density (A cm^{-2}) versus voltage (J–V) relationship. As illustrated in Fig. 5, the regions are: (i) areas in which gold metal is in direct contact with the semiconductor ('MS'), (ii) areas in which gold is on top of the molecular layer, but located near a MS region ('transition') and (iii) areas in which gold is on top of the molecular layer, but far from a MS region ('MMS'). The J–V relationship within a MS region is governed by the TFE model discussed earlier. Atomic force microscopy studies have shown that

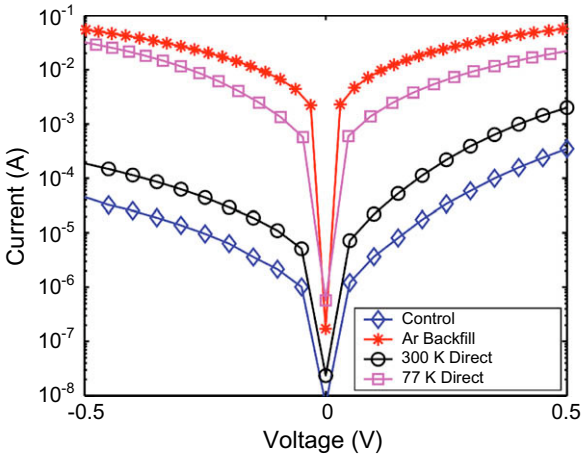

Fig. 3. Representative room temperature (300 K) I–V characteristics for 6 μm diameter devices: Au/p^+-GaAs control sample (blue, diamonds), and samples with Ar backfill (red, stars), and 77 K (pink, squares) and 300 K (black, circles) direct evaporated Au contacts on ODT/p^+-GaAs. (For interpretation of the references to colour in this figure legend, the reader is referred to the web version of this article.)

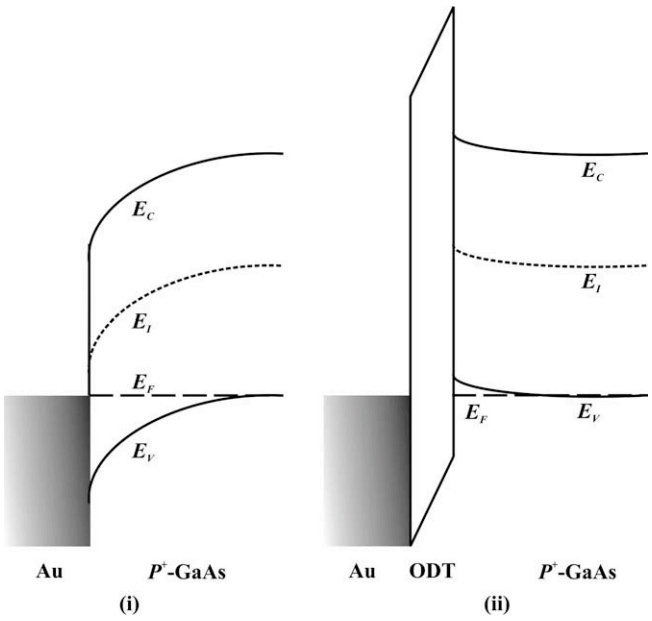

Fig. 4. Energy band diagrams of (i) Au/p^+-GaAs and (ii) Au/ODT/p^+-GaAs devices.

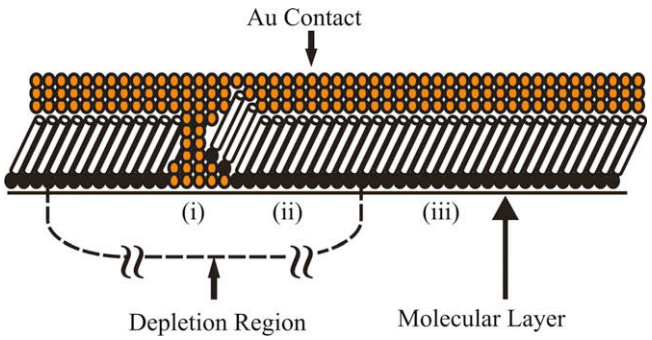

Fig. 5. A schematic of the different conducting regions in Au/SAM/GaAs devices: (i) gold in direct contact with the semiconductor ('MS'); (ii) gold on top of the molecular layer, but located near a MS region ('transition'); and (iii) gold on top of the molecular layer, but far from a MS region ('MMS').

regions of deposited metal penetration through SAMs adsorbed on metals are smaller than the tip dimensions, ~40 nm [32,33]. Areas of Au penetration through the monolayer are therefore considered to be small (diameter ~5 nm) Au/GaAs contacts within the Au/ODT/p^+-GaAs device. The size of the depletion region surrounding such a contact, i.e. the size of the transition region, is estimated to be ~10 nm, based on solution of the 1-D Poisson equation with ADEPT [34] for a barrier height of 0.4 eV and $N_A = 1 \times 10^{19}$ cm^{-3}.

Within an MMS region, the $J-V$ is modified by a number of effects. First, the electrostatic potential is divided between the molecular layer and the semiconductor depletion region, which generally lowers the barrier height between the metal and the semiconductor valence band. Molecular dipoles and semiconductor surface states also modulate the electrostatics. Monolayer disorder induced by the gold deposition would affect both the local electrostatics and the molecular barrier, and therefore the $J-V$ relationship. Finally, the molecular layer introduces an additional barrier with a transmission coefficient which is generally $\ll 1$ and determined by the molecular density of states. For the MMS regions, 1-D electrostatic simulations considering molecular dipoles but ignoring any interface state effects indicate that the semiconductor is close to flat band at equilibrium [22]. Therefore, the $I-V$ characteristics are dominated by the properties of the molecules, and conduction is comparable to that observed in metal–molecule–metal devices. Essentially, the semiconductor contributes a minor amount to the overall barrier, leading to significantly higher currents and smaller rectification ratios. This is consistent with symmetric device behavior predicted by the metal/thin film insulator/metal model developed by Stratton [35]. Symmetric $I-V$s have also been reported for gold–molecule–gold devices using α,ω-dithiol dodecane and dodecanethiol [2]. Based on the relatively high current densities and symmetric $I-V$s observed in Ar backfill and 77 K samples, the conduction in these devices is believed to be dominated by MMS regions. The lower conductance in the 77 K sample is consistent with the larger amount of metal penetration observed in that structure. In this case, a larger fraction of the device area consists of MS and transition regions, which have a lower conductivity.

Within the transition region, the semiconductor surface potential is intermediate between those of the MS and the MMS regions, while the effective transmission coefficient of the molecular layer is comparable to that in the MMS region. In this case, the rectification ratio is expected to be much larger than 1, and the conductance is expected to be significantly smaller than that observed in the MMS region (due to the larger barrier within the semiconductor). The conduction in the 300 K device is believed to consist of current through these transition regions and the MS regions. The conduction through these samples is strongly influenced by a relatively large potential barrier at the GaAs surface and by a large amount of disordering in the ODT SAM induced by the Au evaporation. Further, the relatively large amount of metal penetration observed in the 300 K samples is believed to correspond to a case in which the depletion regions between the areas of Au penetration overlap leading to greatly reduced current flow.

4. Conclusions

In summary, we have shown that the amount of Au penetration through a SAM adsorbed on GaAs can be controlled by varying the substrate temperature and the kinetic energy of the impinging Au. TOF SIMS and IR data indicate that ~4 and ~2 times more gold penetrates through the SAM to the GaAs/S interface after direct evaporative deposition at 300 K and 77 K, respectively, than using indirect (Ar backfill) deposition. The resulting devices have significantly different conductivities: the Ar backfill and 77 K direct deposition samples have ~200 and ~70 times higher conductivity than the 300 K direct deposition samples. Small changes in device structure can therefore lead to very large changes in device conduction. To explain these data, we have developed a model in which these devices consist of three different conducting regions, each with a different $J-V$ relationship.

Acknowledgement

The work was supported by the National Science Foundation under NIRT Grant ECS-0506802 and NASA under URETI Grant #NCC 2-1363.

References

[1] A. Salomon, D. Cahen, S. Lindsay, J. Tomfohr, V.B. Engelkes, C.D. Frisbie, Adv. Mater. 15 (2003) 1881.
[2] J.G. Kushmerick, Mater. Today 5 (2005) 26.
[3] E.G. Emberly, G. Kircenzow, Phys. Rev. B 58 (1998) 10911.
[4] M. Di Ventra, S.T. Pantelides, N.D. Lang, Phys. Rev. Lett. 84 (2000) 979.
[5] S.N. Yaliraki, M.A. Ratner, Ann. N. Y. Acad. Sci. 960 (2002) 153.
[6] P.E. Kornilovitch, A.M. Bratovsky, Ann. N. Y. Acad. Sci. 960 (2002) 193.
[7] C. Grave et al., Adv. Funct. Mater. 17 (2007) 3816.
[8] F. Pauly, J.K. Viljas, J.C. Cuevas, G. Schön Phys. Rev. B 77 (2008). art. no. 155312.
[9] S.N. Yaliraki, M. Kemp, M.A. Ratner, J. Am. Chem. Soc. 121 (1999) 3428.
[10] M. Magoga, C. Joachim, Phys. Rev. B 56 (1997) 4722.
[11] D.Q. Andrews, R.P. Van Duyne, M.A. Ratner, Nano Lett. 8 (2008) 1120.
[12] A. Vilan, A. Shanzer, D. Cahen, Nature 404 (2000) 166.
[13] R.E. Holmlin et al., J. Am. Chem. Soc. 123 (2001) 5075.
[14] M.A. Reed, C. Zhou, C.J. Muller, T.P. Burgin, J.M. Tour, Science 278 (1997) 252.
[15] T. Lee et al., Appl. Phys. Lett. 76 (2000) 212.
[16] W.R. Salaneck, J.-L. Brédas, Adv. Mater. 8 (1996) 48.
[17] R.M. Metzger, T. Xu, I.R. Peterson, J. Phys. Chem. B 105 (2001) 7280.
[18] G.L. Fisher et al., J. Am. Chem. Soc. 124 (2002) 5528.
[19] A.V. Walker, T.B. Tighe, J.J. Stapleton, B.C. Haynie, D.L. Allara, N. Winograd, Appl. Phys. Lett. 84 (2004) 4008.
[20] G. Nagy, A.V. Walker, J. Phys. Chem. B 110 (2006) 12543.
[21] S. Lodha, D.B. Janes, Appl. Phys. Lett. 85 (2004) 2809.
[22] S. Lodha, P. Carpenter, D.B. Janes, J. Appl. Phys. 99 (2006). art. No. 024510.
[23] S. Lodha, D.B. Janes, J. Appl. Phys. 100 (2006). art. no. 024503.
[24] C.L. McGuiness et al., ACS Nano 1 (2007) 30.
[25] C.L. McGuiness, A. Shaporenko, C.K. Mars, S. Uppili, M. Zharnikov, D.L. Allara, J. Am. Chem. Soc. 128 (2006) 5231.
[26] C.L. McGuiness, A. Shaporenko, M. Zharnikov, A.V. Walker, D.L. Allara, J. Phys. Chem. C 111 (2007) 4226.
[27] C. Zhou, A.V. Walker, Langmuir 23 (2007) 8876.
[28] L.H. Dubois, R. Nuzzo, Ann. Rev. Phys. Chem. 43 (1992) 437.
[29] C. Zhou, UV Photopatterning, Electron Beam Lithography and Site-Specific Surface Reactions of Alkanethiolate Self-Assembled Monolayers Adsorbed on Au and GaAs (001), Washington University in St. Louis, St. Louis, 2009.
[30] S.M. Sze, Physics of Semiconductor Devices, John Wiley & Sons Inc., New York, NY, 1981.
[31] F.A. Padovani, R. Stratton, Solid-State Electron. 9 (1966) 695.
[32] C.N. Lau, D.R. Stewart, R.S. Williams, M. Bockrath, Nano Lett. 4 (2004) 569.
[33] Z. Zhu, T.A. Daniel, M. Maitani, O.M. Cabarcos, D.L. Allara, N. Winograd, J. Am. Chem. Soc. 128 (2006) 13710.
[34] J.L. Gray, ADEPT, A Device Emulation Program and Tool, Purdue University, 1995.
[35] R. Stratton, J. Phys. Chem. Solids 23 (1962) 1177.